MICROWAVE MEASUREMENT OF GRAIN AND BIOMASS

A Dissertation
Submitted to the Graduate Faculty
of the
North Dakota State University
of Agriculture and Applied Science

By

Ryan Striker

In Partial Fulfillment of the Requirements
for the Degree of
DOCTOR OF PHILOSOPHY

Major Department:
Electrical and Computer Engineering

July 2022

Fargo, North Dakota

North Dakota State University
Graduate School

Title

MICROWAVE MEASUREMENT OF GRAIN AND BIOMASS

By

Ryan Striker

The Supervisory Committee certifies that this ***disquisition*** complies with North Dakota State University's regulations and meets the accepted standards for the degree of

DOCTOR OF PHILOSOPHY

SUPERVISORY COMMITTEE:

Dr. Daniel Ewert
Chair

Dr. Benjamin Braaten

Dr. Shuvashis Dey

Dr. Xin Sun

Approved:

July 12, 2022 — Date

Dr. Benjamin Braaten — Department Chair

ABSTRACT

Microwave measurement is a powerful method for mass prediction and grain detection. Existing systems are well adapted for small volume grain measurements, but cannot accommodate materials other than grain (e.g. biomass), which are larger in size or dimensional ratios. Therefore, an enlarged measuring system with unique design is needed. This new system's large size improves measurement repeatability by capturing an average response for randomly aligned bulk samples. The system supports homogenous samples up to 0.5 m thick and 1 m square, and it has been validated from 1-50 GHz. By increasing the measurement system's physical size relative to existing systems, it is now possible to measure the plants associated with these grains and seeds in a similar manner. Preliminary results for mixtures of grain and biomass are reported.

Having been validated for grain measurements, the One Meter Fixture is next used to collect phase shift and attenuation data for a variety of grain and oil seed samples (soybean, canola and corn). Using multiple variable linear regression analysis, a comprehensive clean grain mass estimation model was developed based on the dielectric properties of the grain samples derived from the S-Parameters at 13 GHz. Dielectric (ε') constant / properties and phase shift were introduced into the regression models and generated a grain mass estimation result with R^2 values of 0.976, 0.977 and 0.989 for soybean, canola and corn samples, respectively. The results indicate that RF sensing technology has the potential to provide more accurate non-contact sensing methods for estimating grain mass in multiple precision agricultural applications.

ACKNOWLEDGMENTS

Thank you to my adviser, Dr. E., for taking a chance, assembling the team, and turning us loose. Thank you to Dr. Braaten for the funding and administrative support. Thank you to my fellow students: Mary Pearson, Ellen Swartz, Lauren Singelmann, Enrique Alvarez-Vazquez, Henry Wolf, Jared Hansen, Drew Taylor, and Sajid Asif. Thank you to Gurmukh Advani and all the other folks at John Deere for supporting the project and for your engaging comments and questions. Thanks to the NDSU research team: Dr. Dennis Wiesenborn, Dr. Ewumbua Monono, Dr. Harjot Sidhu, Dr. Zhang Yu, Dr. Xin Sun, and Dr. Bingcan Chen. Thanks to Allen Peckrul for all the trips to the greenhouse and research plots, and thanks to Jack Witthauer for all the grain conditioning. Thanks most of all to my wife Jessica, NDSU's original Dr. Striker.

DEDICATION

This work is dedicated to Hazel and Caleb. Stay curious, take risks, keep to the old roads.

TABLE OF CONTENTS

LIST OF TABLES

LIST OF FIGURES

1. MODULAR SYSTEM AND EXPERIMENTAL PROCEDURE FOR MICROWAVE MEASUREMENT OF PLANT MATERIALS AND GRAINS[1]

1.1. Introduction

Microwave measurements of grains or biomass can be useful for mass prediction or for determining material constituents such as water, protein, or oil. Understanding composition is important for proper storage, processing, and market pricing of the material. Microwave measurements can be advantageous compared to other techniques because they are direct, instantaneous, non-contact, and the measurement signal passes through (and characterizes) the entire sample volume rather than capturing only the surface response.

Studying the interaction between biological materials and microwave frequencies for various applications is not a new technique. This technique has been applied extensively to cereal grains, oil seeds, fruits, vegetables, and even meat (Nelson 1973, Trabelsi 2003, Kraszewski and Nelson 2004, Ng, Ainsworth et al. 2008, Clerjon and Damez 2009). Much of the work has been led by United States Department of Agriculture (USDA) scientists Samir Trabelsi and Stuart Nelson in collaboration others. Their work has been focused on saleable commodities such as grains and seeds, and so their free-space measurement system is optimized for small granular materials (Trabelsi 2003). To build on this work, there is now an opportunity to apply microwave sensors earlier in the crop lifecycle by measuring both grain and biomass in the field during growth and harvest. But, this brings new challenges as grains and seeds are intermingled with their plants (biomass). This poses a unique challenge because the geometry of plants is

[1] The material in this chapter was coauthored by Ryan Striker, Yu Zhang, Moruf Disu, Allen Peckrul, Ewumbua Monono, Xin Sun, Bingcan Chen, and Benjamin Braaten. Striker had primary responsibility for all aspects of this chapter.

different than the commodities they produce; plant stalks are larger and longer than seeds. As a first step toward new sensors for in-field use, a new laboratory measurement apparatus is required, one which accommodates a greater variety of materials. This paper is focused on the theory, design aspects, and experimental procedure of a new large-scale laboratory RF fixture referred to as the One Meter Fixture.

Our research interest is to develop and validate a fixture that can collect RF data for both grains and MOG (Material Other than Grain). To construct a free-space fixture capable of measuring MOG, we enlarged the Trabelsi and Nelson (USDA) technique to accommodate larger materials.

1.2. Theory

Key to Trabelsi and Nelson's free-space technique and equations is the fact that, in their words:

information collected is relative to the whole sample volume, thus providing dielectric properties more representative of the sample material. … The two components of the relative complex permittivity … are the average values for the entire sample, assuming the physical properties are the same throughout the sample. (Trabelsi 2003)

Table 1. compares key dimensions of Trabelsi and Nelson's measurement system to those of the new One Meter Fixture. MOG samples inserted into a 25x25x15.38 cm holder would not satisfy the condition of being "the same throughout the sample," for two reasons. First, plant stalks exceeding 25 cm in length would simply not fit into the sample holder. But more significantly, materials with a large aspect ratio (e.g. stalks) would not be free to move/settle into the sample holder uniformly. MOG at odd angles could produce an air cavity whose size is a

large fraction of the total sample. To combat this, the total sample volume was increased ~60x (554k/9k cm3). Antenna spacing was then increased to maintain the far-field condition.

Table 1. Comparison of fixture dimensions

	Trabelsi/Nelson	One Meter Fixture
Antenna spacing	37 cm	109 cm
Sample width	25 cm (transverse)	112 cm
Sample length	25 cm (height)	112 cm
Sample thickness	<15.38 cm	< 5 cm (grain) < 45 cm (MOG)

In addition to enlarging the measurement volume, the system was also rotated 90°. The antennas are pointed up and down rather than sideways. This has the benefit of orienting the sample plane normal to the force of gravity. Samples are arranged on the horizontal support sheet, and any gravity-induced effects do not alter the sample's distribution within the measurement plane. This is in contrast to (Trabelsi 2003) where thickness is controlled by adding/removing foam spacers. Horizontal sample orientation has two related but distinct benefits. In both cases, the benefit derives from the lack of a "bottom" vs. "top" edge of the sample plane. For homogenous samples, it ensures that gravitational force does not cause compression forces across the measurement plane yielding a higher material density at one edge vs. the other. For heterogenous samples, such as a grain MOG mix, it ensures that small grains maintain a uniform distribution within the measurement plane rather than migrating to one edge via settling/sedimentation processes (Cohn 2009, Andreotti, Forterre et al. 2013).

S parameters are measured with a VNA (Vector Network Analyzer). Magnitude and Phase are collected for both S_{12} and S_{21}. From these measurements, the complex permittivity (effective dielectric value) may be derived using the following equations (Trabelsi S 1998).

$$\varepsilon' = \left(1 + \frac{\Phi\lambda_0}{360\mathrm{d}}\right)^2 \quad (1)$$

$$\varepsilon'' = \frac{A\lambda_0\sqrt{\varepsilon'}}{8.68\pi d} \quad (2)$$

Where Φ is the measured S_{21} phase shift, λ_0 is the free-space wavelength, d is the sample thickness, and A is the measured S_{21} attenuation.

1.3. Materials

1.3.1. One Meter Fixture

Structural elements of the measurement fixture are pine lumber, and samples are supported on Owens Corning® FOAMULAR® 150 extruded polystyrene (XPS). These materials are commonly used in building construction, and they were purchased from local hardware stores. Both materials were selected for their low real permittivity (dielectric) values (Knott 1993, Muqaibel, Safaai-Jazi et al. 2003, Waldron and Makarov 2006). Note that the polystyrene sheet is supported by wood only around its perimeter. No wood supports or metal fasteners exist within the center of the antenna pattern. In addition to its use in building construction, polystyrene foam is also commonly found in EMC test chambers where it is used to support electronic devices under test (DUTs) at desired heights above the floor (ground plane) or in particular test orientation (Tas and Pythoud 2017, Pusch, Willenbockel et al. 2019). From an RF perspective, due to polystyrene's low permittivity, the material under test can be treated as if it is suspended in air (Kong, Chung et al. 2003). The polystyrene supporting sheet includes a 5cm tall perimeter wall to prevent small granules from escaping. With respect to strength, the polystyrene sheet has been tested under uniformly distributed loads up to 35 kg. The fixture is modular in design; major vertical/horizontal components are interconnected inside the anechoic chamber with simple wing/thumb screws.

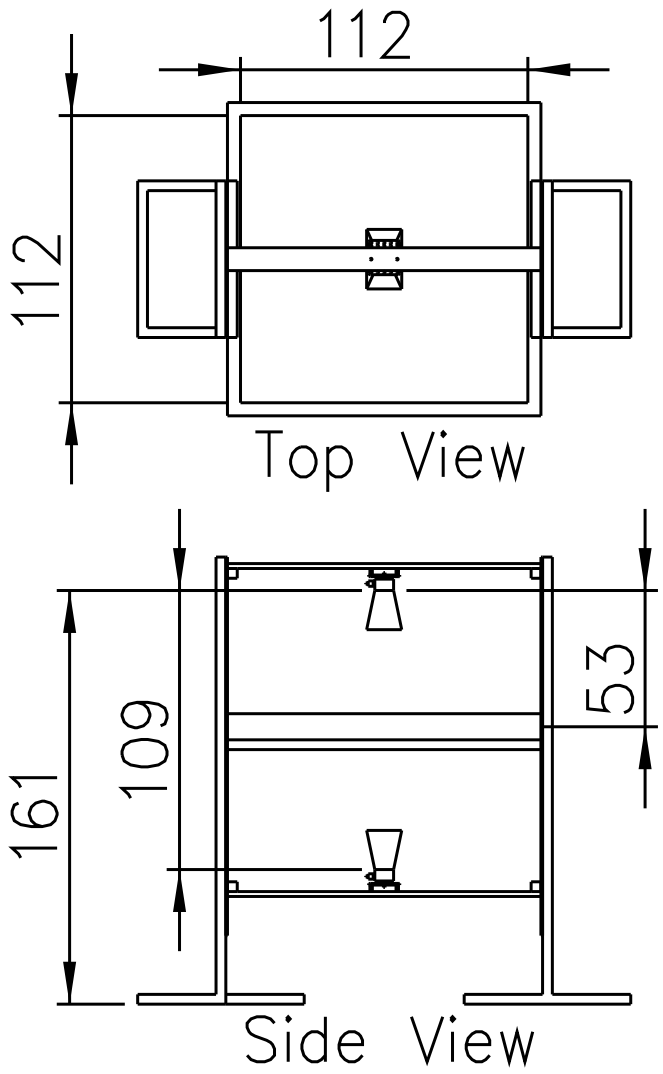

Figure 1. Dimensional drawing of the One Meter Fixture for grain and MOG measurement. Dimensions are chosen to emphasize the space occupied by the material under test and the distance to antennas rather than the construction dimensions of the lumber. All dimensions are in centimeters.

Figure 2. Corn MOG and kernels are shown in the One Meter Fixture.

1.3.2. Reduced Fixture

Though the authors have (hopefully) made a convincing case for the necessity of a One Meter Fixture for experiments involving MOG, such a large fixture is not ideal if experiments are concerned only with grain kernels or ground material. For experiments involving many grain types, it is burdensome to acquire, condition, store, and handle sample quantities sufficient to fill the One Meter Fixture. To quickly adapt/tailor the fixture to different experiments, a reducing insert was created. The insert reduces the sample's length and width to 18" (46 mm) which reduces the sample area by 83%. With the reducer installed, the system is referred to as the Reduced Fixture. The Reduced Fixture retains all components of the One Meter Fixture and simply adds an insert made from XPS, the same air-like material originally used for the sample tray of the One Meter Fixture. The reduced sample area is shown in Figure 3. .

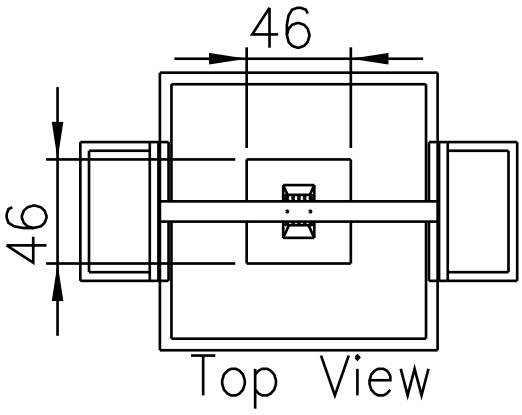

Figure 3. The Reduced Fixture's key dimensions are shown.
The reducer insert can be quickly added to/removed from the One Meter Fixture depending on an experiment's requirements.

As shown in Figure 4. , pyramidal anechoic absorbers surround the sample in the Reduced Fixture and eliminate any RF waves which might otherwise pass around the sample instead of through. Absorbers were not required for this purpose in the One Meter Fixture because the sample size was greater than the antennas' field of view.

Figure 4. Corn kernels are shown in the Reduced Fixture.
Anechoic foam absorbers surround the sample space; note that one absorber has been removed for this photo so that the grain sample can be seen.

As shown in Table 2. the Reduced Fixture allows an experiment with grain depths of 1-4 cm to be conducted with just 6.4 kg of material per sample type; this quantity of material is much more convenient to acquire, condition, store, and handle.

Table 2. Comparison of One Meter vs. Reduced Fixtures

	One Meter Fixture	Reduced Fixture
Antenna spacing	109 cm	109 cm
Sample width	112 cm	46 cm
Sample length	112 cm	46 cm
Sample thickness	< 5 cm (grain) < 45 cm (MOG)	< 10 cm (grain)
Sample area	12544 cm^2	2116 cm^2
Area vs. One Meter	100%	17%
Sample Mass required for depths: 1, 2, 3, 4 cm	9, 18, 27, 36 kg	1.6, 3.2, 4.8, 6.4 kg

In conclusion, researchers may quickly adapt this modular system between the Reduced Fixture configuration for efficient grain-only measurements and the One Meter Fixture configuration for MOG or MOG+grain measurements.

1.3.3. RF Components

Measurements are collected using a Keysight E5071C VNA (300 kHz - 20 GHz). Calibration is performed with the Keysight 85052D kit (DC to 26.5 GHz, 3.5 mm). Two commercial off-the-shelf (COTS) antennas, TDK HRN-0118 (1-18 GHz Horns), are used. The cables are 25 ft (7.62 m) Carlisle (Micro-Coax) UTiFLEX UFA210A with SMA termination on both ends.

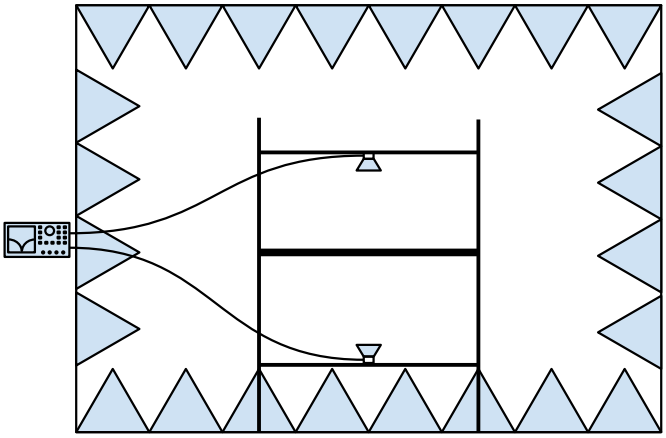

Figure 5. System Connection Diagram. Samples were measured inside an anechoic chamber. Coaxial cables exit the chamber and connect to a vector network analyzer.

1.3.4. Anechoic Chamber

The anechoic chamber's internal size is 2.5 m tall, 3.5 m deep, and 3.5 m wide. The working size of the chamber is reduced by the presence, on all internal surfaces, of pyramidal anechoic foam. Anechoic material is permanently affixed to the walls and ceiling while foam on the floor is mobile. Each foam block is 12 in (0.3 m) tall with a 24 in (0.6 m) square base. The measurement fixture is placed directly onto the chamber floor in the center of the room. As shown in Figure 6. , pyramidal anechoic absorbers are located around and directly beneath the fixture.

Figure 6. The One Meter Fixture is shown with TDK HRN-0118 (1-18 GHz Horns) installed.

1.3.5. Antenna Bracket

One custom metal component is used in the fixture. A ¼" (6.35 mm) thick plate with holes in a 1" (2.54 cm) pattern is used to attach each antenna to the wooden frame. These brackets can be seen in Figure 6. , Figure 7. , and Figure 8. . The bracket can be easily fabricated by cutting and drilling a sheet of acrylic, aluminum, or steel. The bracket is located at the rear of each antenna; the material choice does not alter the antenna's performance. A detailed dimensional drawing of the bracket is available (Weberg and Striker 2020).

1.3.6. Frequency Adaptation

The fixture can also be quickly adapted to measure other frequencies. In Figure 7. , MVG SH5000 horns (5-50 GHz) have been installed. This adaptation is shown to illustrate the fixture's versatility; a full description of the components and procedures used for measurements above 18 GHz is outside the scope of this paper.

Figure 7. The Reduced Fixture is shown with MVG SH5000 (5-50 GHz) antennas installed. In this photo, the antennas are shown with 109 mm antenna-to-antenna spacing.

As seen in Figure 6. , the vertical walls of the fixture are pegboard sheets with holes every 1” (2.54 mm). This allows antenna height/spacing to be quickly altered. For low frequencies, greater spacing ensures the sample is in the far-field (2λ), but closer spacing reduces free space path loss (Balanis 2015). For Reduced Fixture experiments with the MVG SH5000 antennas, antenna-to-antenna spacing has been reduced to 406 mm as seen in Figure 8. .

Figure 8. The fixture supports variable antenna spacing.
Reduced antenna spacing is permitted and advantageous at higher frequencies; revised spacing for 5-50 GHz experiments in the Reduced Fixture are shown.

1.4. Methods

1.4.1. Setup and Calibration

Prior to measurement, sweep settings are configured and two-port calibration is performed. The VNA is configured for 1601 data points and a sweep time of one second. The six reflection calibrations (open, short, load for ports 1 and 2) are completed using standard terminators from the 85052D kit. The transmission (thru) calibration is performed horn-to-horn per Keysight's "Unknown Thru" method (Keysight , Agilent 2006). This calibration technique is chosen so that the VNA measures 0 dB attenuation and 0° phase shift when empty (no grain/MOG) but fully connected. That is, no subsequent data offsets or transformation are required to account for antenna characteristics or path loss.

1.4.1.1. Open Measurement and Dynamic Range

After calibration, the system's dynamic range is characterized by capturing an "open" measurement. One cable is disconnected from the VNA to ensure that thru measurements will

experience 100% attenuation. S_{12} and S_{21} magnitude measurements are captured and stored as "open" measurements. These plots are valuable because the VNA does not report gain of -∞ in this condition. Rather, depending on the losses of the cables and antennas in use, the VNA may report values ranging from -40 to -80 dB at different frequencies. The "open" data set represents the system's dynamic range. By comparing subsequent material measurements against the "open" values, it is possible to detect when a high-attenuation sample has exceeded the dynamic range of the system. This is shown visually in Figure 9. . After the "open" measurements are complete, the cable is reconnected. Proper re-connection is confirmed by verifying thru measurements again yield 0 dB gain and 0° phase shift.

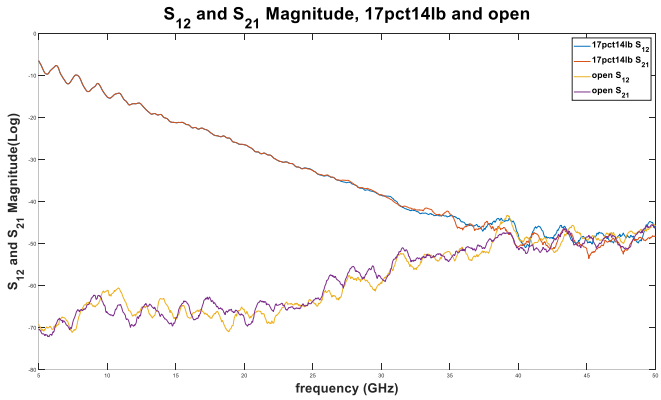

Figure 9. An open measurement is used to determine when a material measurement has exceeded the system's dynamic range.
The upper traces are a material measurement while the lower traces are the open measurement. The material measurement is valid and shows steadily increasing attenuation from approximately 5-35 GHz, but material data is invalid from 35-50 GHz because the measured values are at/near the open plot values.

1.4.2. Material Loading/Unloading

1.4.2.1. Grain Samples

Material is loaded into the fixture with an effort to achieve uniform sample thickness while fully spreading material to the extents of the support tray's depth and width respectively. When loading small granules, a stick or other short length of material is used to distribute and

smooth the material (see Figure 10.). Then, sample thickness and uniformity are verified at several points with a ruler or caliper (see Figure 11.).

Figure 10. Granular material is smoothed/leveled by hand

Figure 11. A caliper's depth rod is used to verify uniform material depth (thickness) within the fixture.

Many experiments involve the incremental addition of material; subsequent data analysis is easier when the measurements are based on quantities 1x, 2x, 3x, and 4x. For these scenarios, material is added by mass rather than volume or thickness (see Figure 12.). Though all three factors are theoretically equivalent for a bounded tray of this type, mass is the most repeatable and straightforward to measure during the experiment.

Figure 12. Mass was used for experiments requiring incremental addition of equally sized portions.

Materials are not deliberately compressed/compacted within the fixture. The materials maintain their position in the fixture because the sample tray is flat (normal to gravity).

1.4.2.2. MOG Samples

MOG samples vary widely both in their source and their characteristics. MOG obtained from combine discharge (residual material) is often dimensionally small due to deliberate cutting and threshing in the machine. Residue also tends to be dry both because fresh green MOG can clog equipment and because producers would prefer to field-dry grain (and therefore MOG) rather than incurring the additional costs associated with post-harvest drying. An example of collecting combine residue is shown in Figure 13. .

Figure 13. A tarp is used to capture wheat residual material as it is discharged from the rear of a plot combine.

Figure 14. Wheat MOG (combine residue) is shown in the One Meter Fixture.

If MOG is desired at higher moisture levels (green MOG) and/or un-threshed (whole plants), then plants may be hand-cut in the field (Figure 15.) or greenhouse(Figure 16.). Field and greenhouse plants are often available during alternate seasons. Greenhouse plants tend to be smaller (less mature) and greener (higher moisture content). Hand-harvested plants allow the

researcher maximum control over the MOG condition; one disadvantage of hand-harvesting plants is the need to remove grains manually (Figure 17.).

Figure 15. Mature but green barley was hand-cut to obtain whole plants at an above-average moisture level.

Figure 16. Immature wheat plants are hand-cut in a greenhouse.

Figure 17. Grain heads must be manually removed from hand-cut plants. In this photo, wheat heads are removed from greenhouse plants.

Because of MOG's low material density and packing density, fewer thickness levels are practical in the One Meter Fixture. Similar to the grain method, MOG samples are most accurately characterized by their mass with thickness as a second correlated measure.

1.4.2.3. Carriers and Liners

To assist in loading/unloading materials, a carrier/liner may be used. Craft paper (see Figure 2.) and polyethylene tarpaulins (see Figure 14.) have each been used. Because these carriers are thin, non-polar, and low-dielectric they have a negligible effect on the resultant measurements.

For small granular materials such as corn starch or canola seeds, a paper liner aids in removing 100% of the sample from the fixture. Once the majority of a sample has been scooped out of the fixture, the paper liner can be carefully raised and folded into a funnel to pour the sample residue back into its container.

For MOG only experiments, the major benefit of carrier sheets is the ability to apportion the material prior to entering the anechoic chamber. Handling of MOG inside the chamber should be minimized because stray debris can quickly dirty floors and become lodged in the crevices of pyramidal absorbers. Using a tarp, MOG samples can be apportioned either outdoors or in a shop/garage space. In addition to keeping the chamber clean, tarps also allow experiments to be conducted more quickly. Tarp edges can be quickly gathered/rolled up, similar to a taco or burrito, to transport MOG. MOG rolled inside a tarp can be easily transported in a vehicle, carried through doorways, and placed into the measurement fixture without loss of material. Once the material is in the fixture, the tarp is unrolled, and measurements are collected. Following measurements, the material can be quickly removed by again gathering up the tarp edges as before. A single MOG sample may be inserted/removed from the chamber several times in the course of an experiment for reasons such as collecting technical replicates, measuring sample combinations (e.g. MOG sample 1 stacked atop MOG sample 2), or to measure the same sample at different moisture levels (sample is transported to a drying facility).

It is noted that tarps often include metal grommets at the corners/edges. These do not affect measurements because they are outside of the antenna's field of view.

1.4.3. Data Capture

Complete two-port S-parameters are stored for each material type and amount. This includes both magnitude and phase values for S_{11}, S_{21}, S_{12}, and S_{22}. Magnitude data is stored as gain (negative values) in the Log Mag (dBm) format. Phase data is stored in the Unwrapped Phase format (degrees). Unwrapping the phase aids in examining intra-sample phase shift (e.g. phase shift at 3 vs. 10 GHz). To allow for inter-sample comparison of phase measurements, it is

necessary to ensure that all captures share a common 0° point. Because phase shift and frequency are proportional, it is most convenient to capture phase data with ~0° phase shift at 0 Hz.

1.4.4. Moisture Conditioning

Grain acquired through normal distribution channels commonly possesses very low moisture. For RF experiments considering the effect of moisture, grains may be conditioned to higher moisture levels by first adding relatively small amounts of water, then mixing the sample thoroughly, and finally storing at refrigerator temperatures for at least 24 hours. To achieve very high moisture levels, the process of adding water, mixing, and cold storage may need to be repeated multiple times. Germination is the limiting factor to consider when conditioning grain to high moisture levels.

Unlike grain, re-hydrating MOG is impractical. Whereas grain kernels simply swell/contract as moisture rises/falls (within limits), dry stalks and leaves do not readily reabsorb water. Therefore, MOG experiments interested in moisture content are advised to begin with high moisture (green) MOG and collect data at various stages of dehydration.

MOG dehydration can be slow and inconsistent if material is simply lying atop an impervious surface in the climate-controlled environment of a chamber. MOG may be dried more quickly and uniformly in off-site facilities as shown in Figure 18. and Figure 19. .

Figure 18. MOG is passively dried in a greenhouse. For drying, MOG is transferred from air-impervious tarps to open-mesh fishnets.

Figure 19. Purpose built drying rooms consist of a perforated floor, a heat source, and a fan. Heated air is blown up through the floor; the air temperature and flow rate can be controlled.

1.5. Results

It should first be noted that the focus of this manuscript is the fixture and method. These are described in detail to aid others wishing to reproduce or extend the work and for the authors' citation in future works focused on measurements, modeling, and conclusions using this method. Measurement results presented herein are intended to show that the method is repeatable and conforms to the underlying assumptions and predictive equations of Trabelsi and Nelson.

1.5.1. One Meter Fixture Validation

In (Trabelsi 2003), several linear relationships are demonstrated. First, greater phase shift is expected at higher frequencies. The slope down and to the right for each individual data series in Figure 20. shows agreement with this relationship. Next, (Trabelsi 2003) showed increasing phase shift with increasing material depth. In Figure 20. , the data series are labeled by mass (weight), but this corresponds directly to depth since the material is contained within a bounded area. Thus, Figure 20. also shows agreement with (Trabelsi 2003) because the stacking the data series is according to depth (weight); the lowest depth (weight) has the lowest phase shift values and the greatest depth (weight) has the largest phase shift.

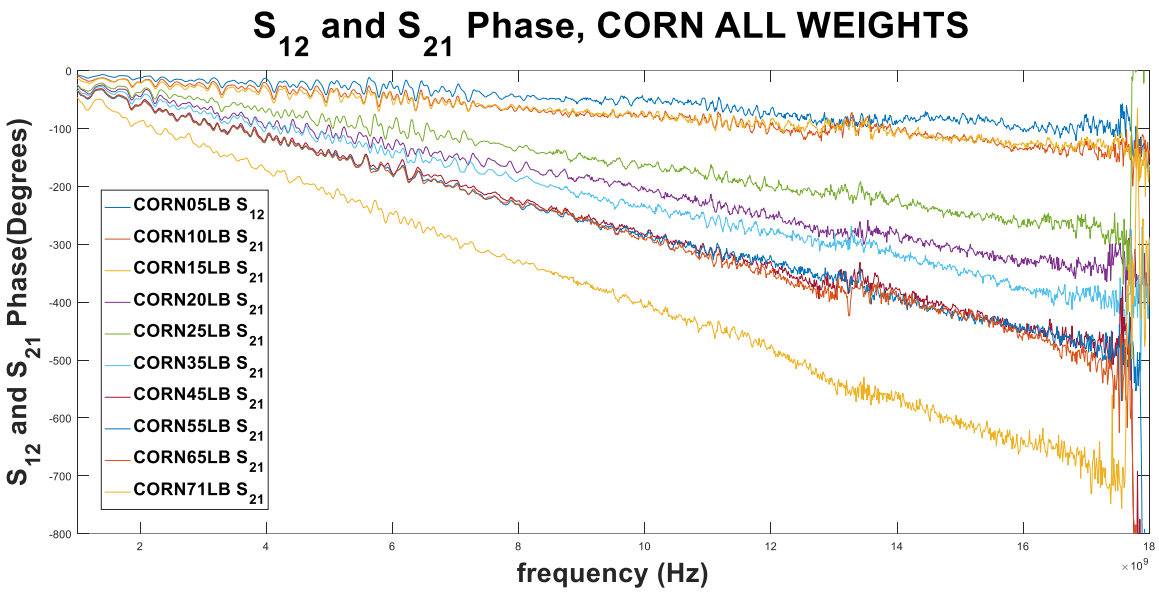

Figure 20. Graph of S_{21} phase shift vs frequency for whole kernel corn of various sample sizes in the One Meter Fixture.
Corn kernels were from the same batch and were stored at ambient temperature and humidity. As expected, phase shift increases with both frequency and mass (depth) of material.

1.5.2. Reduced Fixture Validation

To validate the Reduced Fixture, corn kernels were again measured at increasing depths and the data examined for the same two trends: phase shift increases with frequency, and phase shift increases with depth. Both of these trends can be seen in Figure 21. ; note that a Savitzky-Golay filter has been applied in this case.

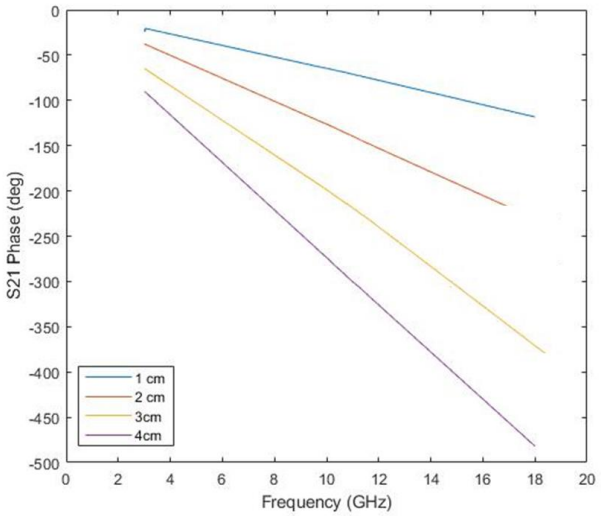

Figure 21. Graph of S_{21} phase shift vs frequency for whole kernel corn of depths 1-4 cm in the Reduced Fixture.
Data has been smoothed using a Savitzky-Golay filter. Corn kernels were stored at ambient humidity and temperature; kernel moisture content was measured as 8.7%. As expected, phase shift increases with frequency and with depth of material.

1.5.3. MOG Measurements

1.5.3.1. MOG Depth

Having validated the fixture using grain samples, cursory experiments were then conducted relevant to the original purpose: measurements with MOG. The graphs of 0 examine the effect of MOG depth for samples containing both wheat kernels and wheat MOG. The same linear relationship between depth and phase shift previously seen in grain kernels is now shown for MOG; that is, increasing the depth of MOG produces proportional increases in phase shift. As the graphs contain both grain only as well as grain+MOG, the phase shift arising from each may also be compared. Notably, 30 cm of MOG produces a phase shift equivalent to just 0.75 cm of grain in this case (MOG moisture = 9%, grain moisture = 14%.

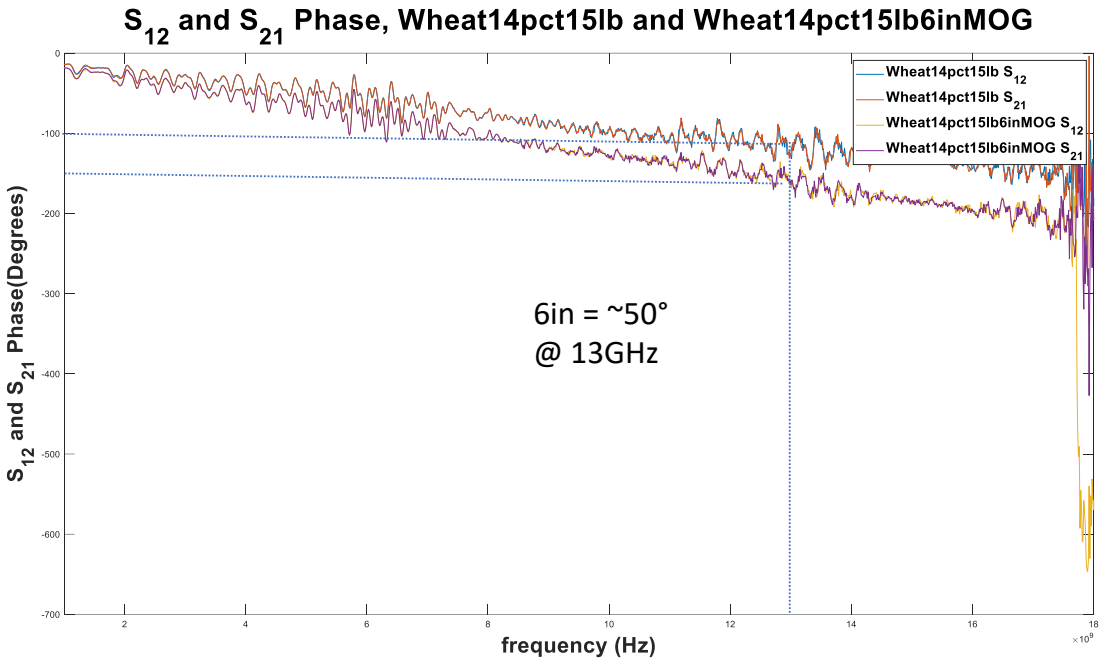

(a)

Figure 22. S_{21} phase shift vs frequency is shown for combinations of wheat kernels and MOG. The thickness of MOG is varied between the three images: 15, 30, and 45 cm (6, 12, and 18 inches) for images a, b, and c respectively. The quantity of wheat kernels was constant across the three images: 6.8 kg (15 pounds) corresponding to ~0.75 cm depth. Moisture content was 14% for wheat kernels and 9% for MOG. In each graph, a plot of grain only (no MOG) is compared to a plot of grain + MOG.

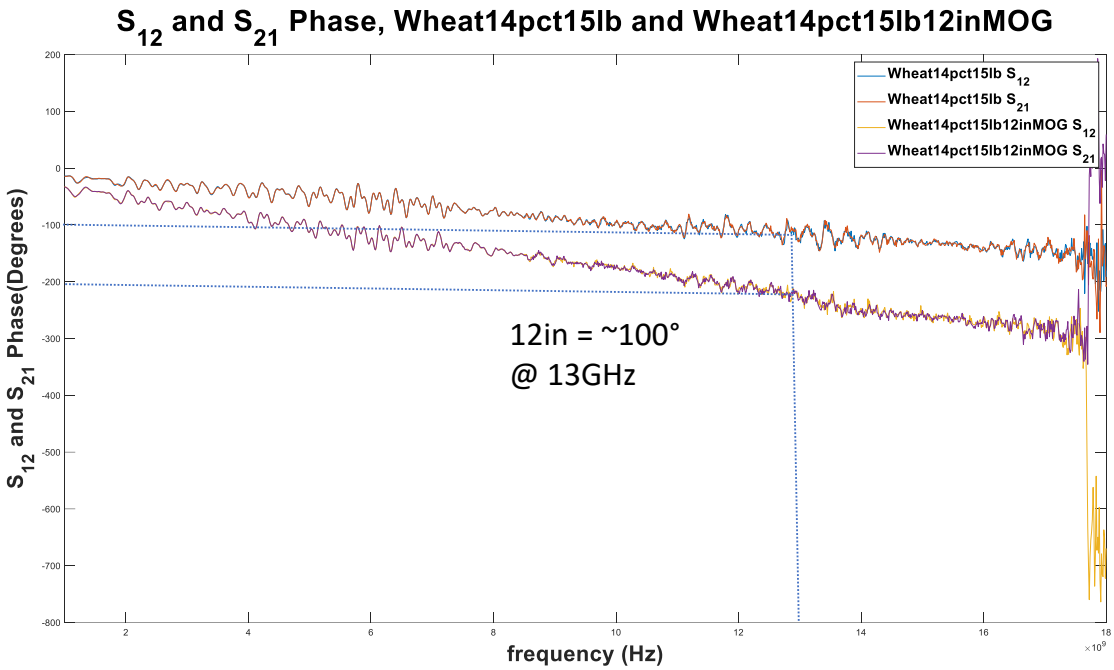

(b)

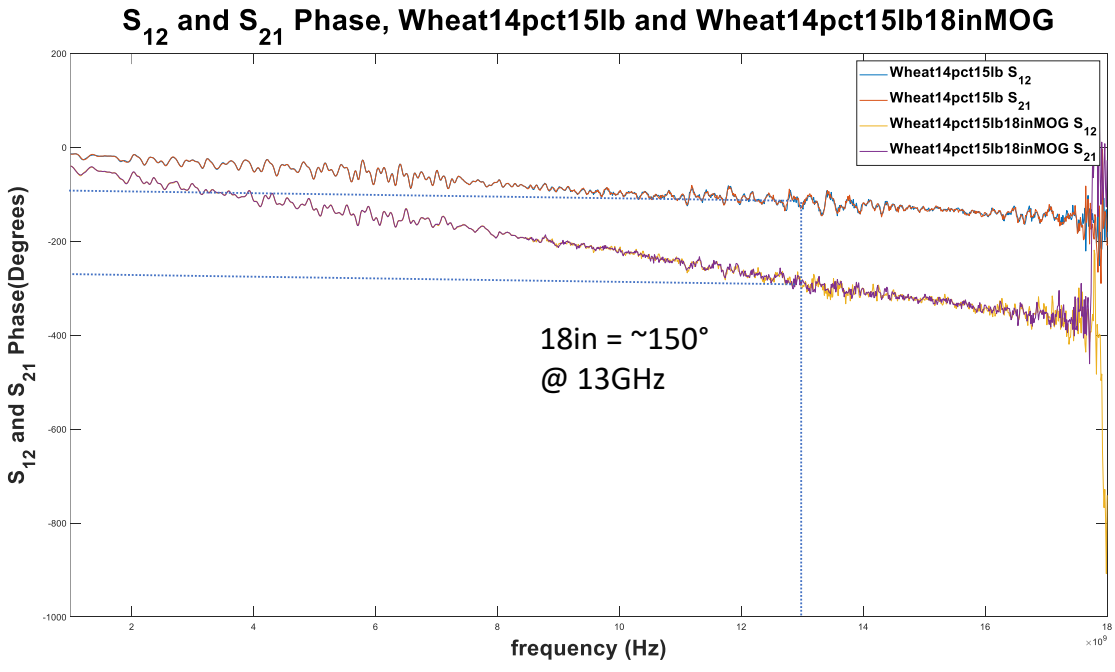

(c)

Figure 22. S_{21} phase shift vs frequency is shown for combinations of wheat kernels and MOG (continued). The thickness of MOG is varied between the three images: 15, 30, and 45 cm (6, 12, and 18 inches) for images a, b, and c respectively. The quantity of wheat kernels was constant across the three images: 6.8 kg (15 pounds) corresponding to ~0.75 cm depth. Moisture content was 14% for wheat kernels and 9% for MOG. In each graph, a plot of grain only (no MOG) is compared to a plot of grain + MOG.

1.5.3.2. Detecting Kernel Moisture in the Presence of MOG

0 examines whether the presence of MOG confounds the detection of differing grain moisture content. The three graphs show plots for two grain samples, having 14% and 17% moisture content. Grain quantity for both samples is 6.8 kg (15 pounds) corresponding to ~0.75 cm depth. MOG depth is varied across the graphs: 15, 30, and 45 cm (6, 12, and 18 inches). MOG moisture content was 9% in all cases. For all three graphs, the 3% difference in grain moisture is discernable.

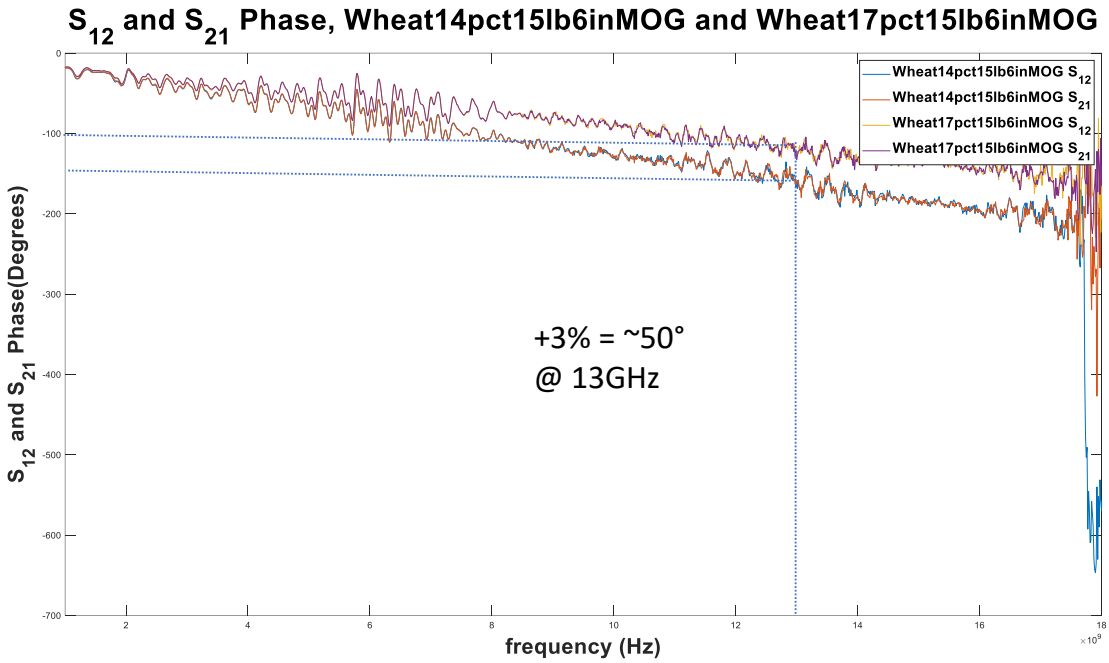

(a)

Figure 23. The three graphs above each plot two grain samples, having moisture contents of 14% and 17%.
The MOG depth (thickness) is varied between the three graphs: 15, 30, and 45 cm (6, 12, and 18 inches) in images a, b, and c respectively. The 3% change in grain moisture content can be clearly seen in (a) and remains distinguishable in (b) and (c).

(b)

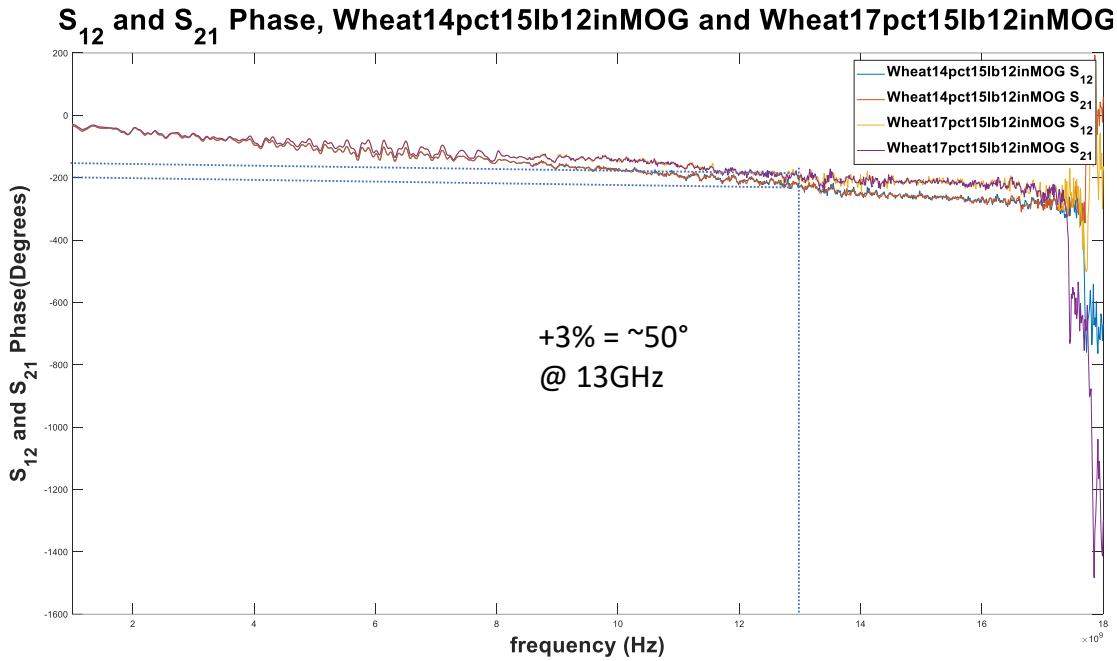

(c)

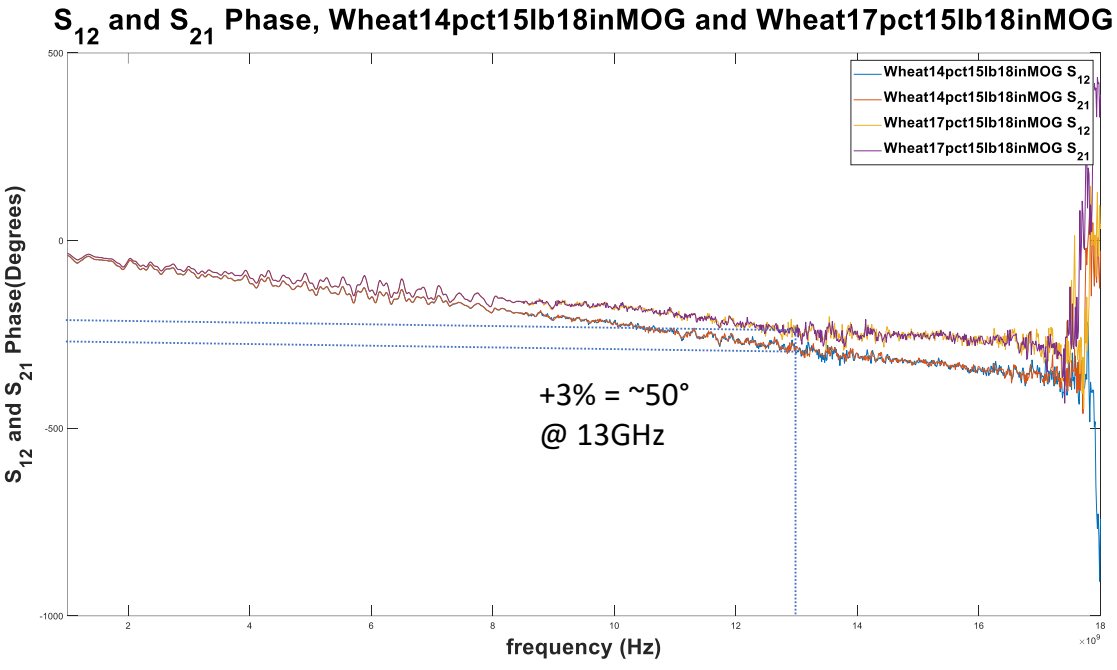

Figure 23. The three graphs above each plot two grain samples, having moisture contents of 14% and 17% (continued). The MOG depth (thickness) is varied between the three graphs: 15, 30, and 45 cm (6, 12, and 18 inches) in images a, b, and c respectively. The 3% change in grain moisture content can be clearly seen in (a) and remains distinguishable in (b) and (c).

1.5.3.3. Detecting grain depth in the presence of MOG

Figure 24. examines whether the presence of MOG confounds the detection of differing grain depths. With all other factors held constant, grain depth is varied by 0.25 cm in (a) and 0.75 cm in (b). In both cases, the change is discernable.

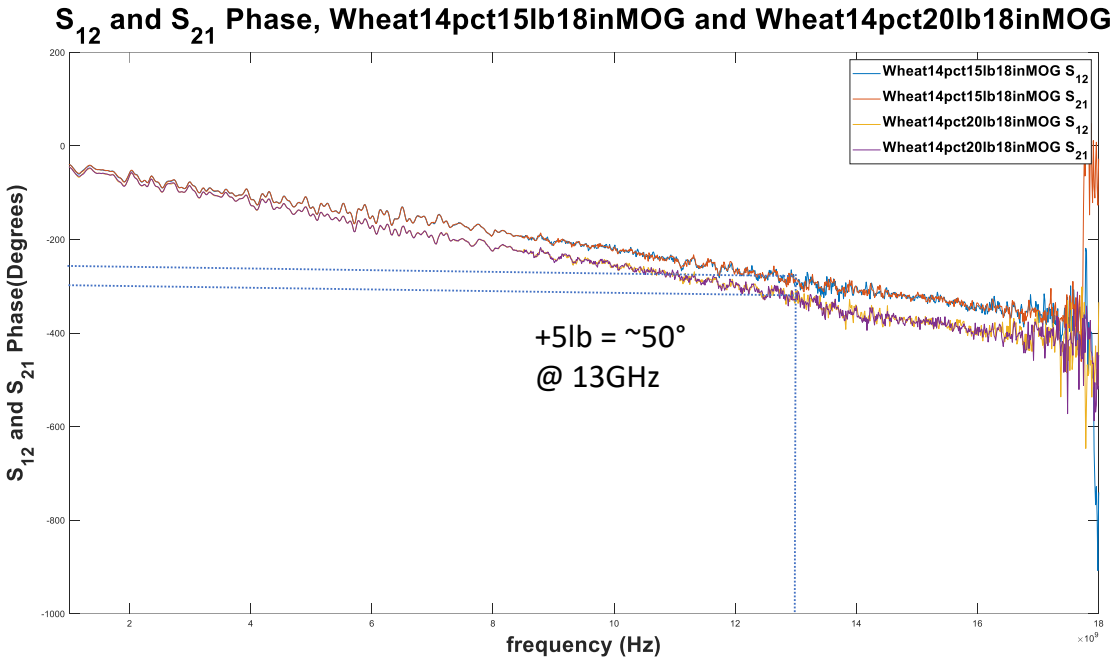

(a)

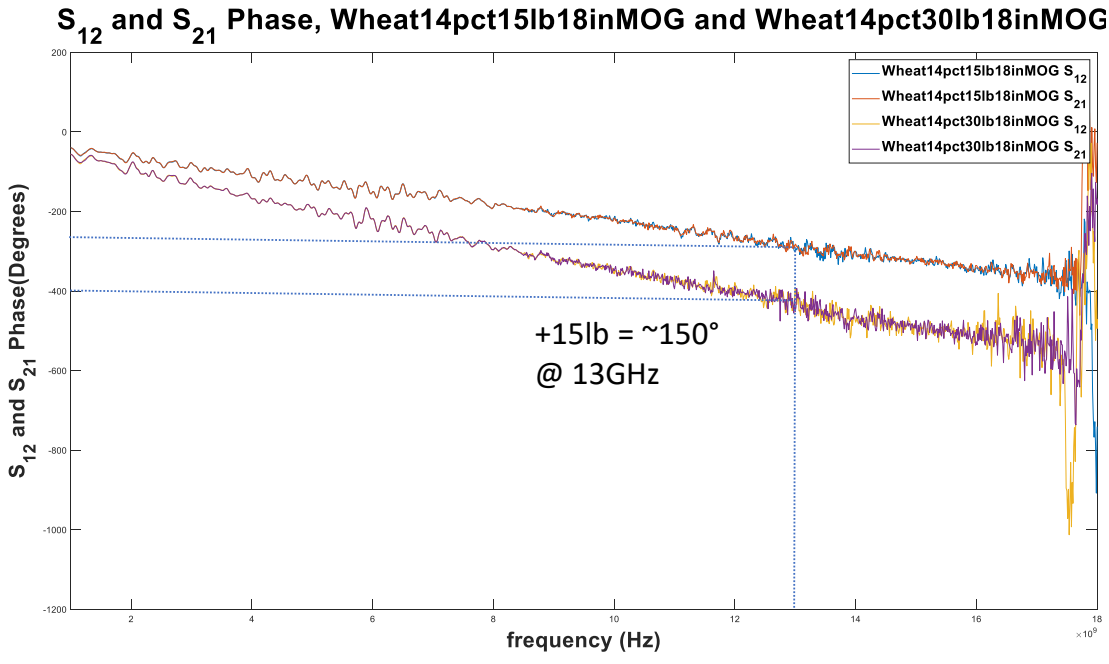

(b)

Figure 24. In the two graphs above the depth of grain is varied.
In (a), grain depths of 0.75 and 1.0 cm (6.8 and 9.0 kg or 15 and 20 pounds) are compared. In (b), grain depths of 0.75 and 1.5 cm (6.8 and 13.6 kg or 15 and 30 pounds) are compared. Grain moisture content was 14% in all cases. MOG depth is 45 cm (18 inches) with moisture content 9% in all cases.

The preliminary results of 0, 0, and Figure 24. show that MOG and grain can be measured together in the One Meter Fixture. Discernible changes in phase shift are associated with changes in MOG depth, grain kernel depth, and grain kernel moisture content. A confounding factor is that these three experimental variables give rise to the same 50° change in measured S_{21} phase shift: 15 cm (6 inches) change in MOG depth, 0.25 cm (2.2 kg or 5 lb) change in grain depth, or 3% change in grain kernel moisture content.

1.6. Conclusions

In conclusion, both the One Meter Fixture and Reduced Fixture have been validated against prior studies based on grain measurements and S_{21} phase shift measurements.

Furthermore, the fixture has been shown to fulfill its original purpose; it accommodates MOG samples in addition to grain. Preliminary data suggests that multiple experimental factors contribute to the same measurement parameter: S_{21} phase shift. Further investigation will be required to determine whether these factors can be separated or distinguished from one another.

As previously described, the materials for the One Meter Fixture can be purchased from any local building supply store. No custom parts or expensive tooling are required for others wishing to reproduce this fixture for their own large-format material measurements.

Paired with appropriate horn antennas, the fixture supports broadband characterization of a wide range of agricultural materials. This broadband laboratory characterization is a useful first step toward in-field sensing of grain and MOG.

2. DIELECTRIC CONSTANT-BASED GRAIN MASS ESTIMATION USING RADIO FREQUENCIES SENSING TECHNOLOGY[2]

2.1. Introduction

Yield monitoring is an important aspect of modern precision agriculture applications. According to a survey conducted in the year of 2019 by Purdue University in precision agriculture, 71% of dealers are offering or will offer a yield monitor service in the next 3 years (Erickson and Lowenberg-DeBoer 2019). The survey also indicated that yield monitoring ranked first place (69%) among all the different precision agriculture technologies among farmers to adopt in their operations.

A typical yield monitor system includes measurement of grain information such as grain flow, grain moisture, area covered and location. The key component for measuring grain flow is a sensor installed on the combine harvest system called the grain/mass or volume flow sensor. Depending on the principle of measurement, the flow sensor includes mass flow sensor and volume flow sensor. For the mass flow sensor, sensing techniques and sensor location are two main factors affect the accuracy. Most commercial mass flow sensors are based on impact-type sensing technology, in which the sensor location and the instrument inclination resulted in the measurement errors (Fulton, Sobolik et al. 2008). In addition, grain moisture content dominates the weight per time in mass flow and affects the measurement accuracy largely. Some reported research showed the mass flow sensor error could be up to 23% due to the large grain moisture content and the location of the sensor mounted on the machine(Chung, Choi et al. 2016). For

[2] The material in this chapter was coauthored by Yu Zhang, Ryan Striker, Moruf Disu, Ewumbua Monono, Allen Peckrul, Gurmukh Advani, Bingcan Chen, Benjamin Braaten, and Xin Sun. Striker had primary responsibility for the design of the laboratory a and data collection.

volume flow sensor, it measures the height of grain flowing through the optic sensors in a fixed time interval. The measured height was converted to volume and mass eventually. Grain moisture content, physically asymmetric feeding on the elevator and the location of the sensors affected the grain estimation accuracy utmost (Strubbe, G., 1996). The third one is the impact sensor, which is one of the most popular commercial sensors. The calibration of this sensor was affected by the slope of the field. John Fulton(2008) investigated different impact sensors at different moisture content under varying field slope conditions. His evaluation indicated that a small variation in moisture content made it difficult to assess the calibration factors for impact-type sensors. Besides, grain properties including moisture content, friction, and kernel size and the varying flow rate are the main causes for the accuracy reduction (Arslan, S. et al.,1998). Schrock (1995) developed a triangle elevator measured grain flow at different moisture content. His research demonstrated that grain moisture content contributes large effects on mass flow sensing. Over the years, researchers have investigated different sensing technologies, including radiometric, x-ray and optical light, to diminish the effects of moisture content and slope of the field and further explore the possibility of increasing the yield monitoring prediction accuracy (Tucker, Elgin Jr et al. 1979, Arslan, Inanc et al. 2000, Thomasson, Sui et al. 2006). Therefore, a sensing technology which is sensitive to grain moisture content and not limited by physical properties of measurement (machinery vibration, field slope, and grain kernel size, etc.) is necessary to improve the grain mass estimation accuracy.

In recent years, researchers have used Radio Frequency (RF) sensing technology in many different industry applications which include communications based on 5G millimeter wave system (Kim and Kim 2021), ranging and detection (RADAR) (Kadwane 2021), healthcare (Shah and Fioranelli 2019, Shah, Abbas et al. 2021), chemical detection (Chen, Stewart et al.

2015), language recognition (Crawford, Aksu et al. 2020) and food quality evaluation (Awuah, Ramaswamy et al. 2005). RF sensing technology also plays an important role in the agriculture industry, specifically in grain and soil moisture content prediction (Nelson 1987, Nelson, Trabelsi et al. 2001, Josephson, Barnhart et al. 2019). In Nelson's research, RF sensing technology has been used to measure grain dielectric properties in the frequency range from 250 Hz to 12.1 GHz at the moisture contents ranging from 2.7% to 23.8% (wet basis) (Nelson 2015). Nelson indicated that RF sensing is a powerful tool to estimate grain moisture contents in terms of agricultural application. His experiments have been conducted on unshelled peanuts and kernels (shelled peanuts) for moisture contents between 6% and 22% at the frequency range from 6-18 GHz at 23˚C temperature (Trabelsi and Nelson 2005) . However, limited research used RF sensing technology for grain mass evaluation with an industry-satisfied prediction model.

In this study, the objective is to use RF sensing technology to measure mass attributes for three different types of grain (soybean, canola and corn), and establish a mass estimation model using statistical analysis. The results from this research will provide an innovative sensing method for grain mass estimation in multiple agricultural applications.

2.2. Materials and Methods

2.2.1. Grain Sample Preparations and Constituent Analysis

Approximately 330 lb of soybean, canola, and corn were purchased from elevators across North Dakota. The samples were kept in totes in the cold room at 4˚C until they were conditioned at different moisture levels. Approximately 15 lb samples for each grain were conditioned to moisture contents between 8-27%. Table 3. shows the target moisture contents for the different grains. Conditioning of the grains to the target moisture content depends on the initial moisture content of the grains. In case the target moisture content was lower than the

initial moisture content of the grain, the 15 lb sample was dried in an oven at 30˚C equipped with a fan blowing air through the grain at 0.014 m^3 per min. The moisture content of the sample was checked every 2 h until the target moisture content was attained. The moisture contents of the seeds before and after conditioning were measured using an electrical capacitance grain analyzer (DICKEY-John GAC 2100). In case the target moisture content was lower than the initial moisture content, the amount of water to be added was calculated. The grain samples were conditioned in a 99 L concrete mixer (Harbor Freight, Fargo ND) bought for such purpose. The calculated amount of water was added slowly into the mixer. After mixing for approximately 10 mins, the conditioned samples were put in 19 L pails and stored in the cold room for 48 h. The moisture contents of the conditioned samples are checked using a moisture analyzer before any RF measurements.

The oil content for the canola sample was analyzed by quantifying the amount oil extracted with n-hexane using an accelerated solvent extraction unit (ASE 200, Dionex Corp; Sunnyvale, CA, USA). Approximately 4 g of the sample and 3 g of diatomaceous earth were ground in a brim coffee grinder. The ground sample in triplicate were put in ASE cells. The extractions were performed at 100 °C and 6.7 MPa with a 5 min equilibration time and triple sets of 10 min static cycles with 100% flush volume and 60 s spurge time with industrial-grade N_2. The extracted fractions were automatically collected in pre-weighed vials, and n-hexane solvent was evaporated using a stream of dry air (−70 °C dew point). The vials with oil were dried overnight in a vacuum oven at 40 °C and 90 kPa vacuum pressure. The total oil content from different replicates was recorded.

Crude protein was determined by Dumas combustion method based on each of their N% (using a LECO FP428 nitrogen analyzer (LECO Corporation, St Joseph, MN, USA). A total

starch assay kit K-TSTA-50A (Megazyme International) was used to determine the starch content following the AACC International Approved Method 76–13.01.

2.2.2. Static Measurements of Clean Grain Mass Using RF Sensor

In this experiment, a Keysight E5071C ENA Series Network Analyzer (300 kHz-20 GHz) and a pair of TDK HRN-0118 Horn Antennas (1-18 GHz) were used to collect S-parameters (S_{11}, S_{22}, S_{12}, S_{21}) in a range of 300 kHz to 20 GHz. Both magnitude (in dB) and phase shift (in degrees) were measured at 1601 data points resolution within 1s scan duration. A transmission calibration was performed with horn antennas attached. To reduce ambient noise interference to the RF signal, the measurement was conducted on a static test bed placed inside an anechoic chamber at NDSU Electrical and Computer Engineering Department. The anechoic chamber walls, ceiling and floor are lined with pyramidal Radiation Absorbent Materials (RAM). A static test bed was developed by Ryan Striker to conduct RF data collection, shown in Figure 25. The sample holder on the static test bed was made of extruded polystyrene foam and surrounded with RAM to further reduce signal reflections. The fixed surface area of the sample holder was measured to be 2,090 cm^2 (45.9x45.9cm). Samples vary in thickness; the sample volume may be calculated as thickness * surface area (thickness * 2090). A data at “Empty” scenario, with no sample loaded on the test bed, was collected each time before sample measurement to reduce the error and differences among measurements. In data collection, different quantities (mass/thickness) of each sample type were placed in the sample holder. Details on the characteristics and measurements of the sampled grains are shown in Table 3. For all commodities, samples were measured in increments of 1 cm thickness (3.5 lb mass). For canola, additional measurements were taken at intermediate ½ cm (1.75 lb) points.

Table 3. Characteristics of different grain samples used to collect RF data

Samples	Dominant components and contents (%)	Sample thickness (cm)	Moisture content (%)	Grain mass (lb)
Canola	Oil – 41%	1, 1.5, 2, 2.5, 3, 3.5, 4	8, 11, 14, 17	3.5, 5.25, 7, 8.75, 10.5, 12.25, 14
Soybean	Protein – 38%	1, 2, 3, 4	8, 10, 12, 14,16	3.5, 7, 10.5, 14
Corn	Starch – 69%	1, 2, 3, 4	12, 17, 22, 27	3.5, 7, 10.5, 14

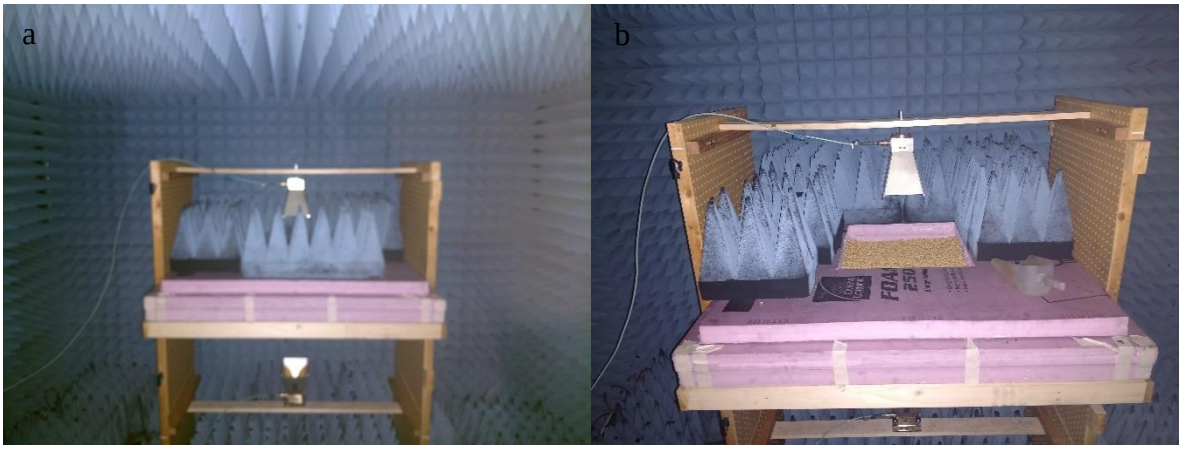

Figure 25. Anechoic chamber and static test bed for data collection
(a) Anechoic chamber and static test bed (b) One piece of RAM has been removed to reveal the sample cavity.

In this study, phase shift ($|S_{21}|$) at 13 GHz and dielectric constant (derived from S parameters), were used in the grain mass estimation model. The phase shift at lower frequencies is smaller, while at higher frequencies, as we approached the limit of our equipment's operating range, the signal occasionally became volatile and unstable due to the limitation of the equipment measurement range. Therefore, phase shift at 13 GHz, which is in the middle of our equipment measurement range with less noises, was selected in this research for the grain mass prediction model. Phase shift ($\angle S_{21}$) and magnitude of the transmission loss ($|S_{21}|$) from 3-16 GHz were used to calculate dielectric constant in the grain mass prediction model, based on Nelson's research on free-space transmission techniques (Trabelsi 2003). All the data points were denoised using Savitzky-Golay methods (Mario A. de Oliveira 2018). Assuming the

physical properties of the grain samples are evenly distributed throughout the samples, the dielectric constant and loss factor were calculated using the equations as follows (Trabelsi S 1998):

$$\varepsilon' = [1 + \frac{\emptyset * \lambda_0}{360d}]^2 \quad (3)$$

$$\varepsilon'' = \frac{A * \lambda_0}{8.686\pi d}\sqrt{\varepsilon'} \quad (4)$$

where $\lambda_0 = \frac{c}{f}$ is the wavelength in free space, *c* is speed of light and *f* is frequency ranged from 3-16 GHz, *A* is attenuation in dB and $\emptyset$ is phase shift in degrees. In this experiment, the VNA was configured to capture the unwrapped phase; it was not limited to [-180˚ 180˚]. A multiple linear regression model of dielectric properties is necessary for the grain mass prediction model. Outlier analysis was conducted prior to regression analysis.

2.2.3. Model Development

For model development, a multiple linear regression method was applied to estimate the clean grain mass. The procedure was conducted using SPSS software (IBM SPSS Statistics for Windows, Version 25.0. Armonk, NY: IBM Corp.).

$$mass = A_0 + a * phase + b * \varepsilon' \quad (5)$$

Where *mass* is the estimated grain mass, in *lb*, A_0 is the intercept at phase shift = 0, ε'=0, and *a* and *b* are the parameters determined by the regression.

2.3. Results and Discussions

2.3.1. Correlations and Significance Analysis of Independents in Linear Regression Model

In this study, phase shift, moisture content, and dielectric properties (ε' and ε'') were the main parameters to be considered in the procedure of the linear regression estimation model development. Statistical correlation analysis and significance analysis were conducted to select the most significant parameters for modeling. The correlation results in Table 4. showed that all

three grain samples, phase shift was statistically correlated with grain mass. Dielectric constant, (ε') and loss factor, (ε'') were both correlated with grain mass at fairly low level but correlated with moisture content at high level, which meant both ε' and ε'' were valid indicators to reflect moisture variations in the estimation model (Soltani and Alimardani 2014, Trabelsi, Mckeown et al. 2016).

Table 4. Correlation analysis of independence for grain mass model (soybean, canola and corn)

		Phase shift	ε'	ε"	MC
Soybean	Mass	-0.932**	0.243	0.034	0.000
	Phase shift		-0.553*	-0.252	-0.246
	ε'			0.685**	0.657**
	ε"				0.793**
Canola	Mass	-0.926**	0.005	0.054	0.000
	Phase shift		-0.355**	-0.360**	-0.330*
	ε'			0.837**	0.908**
	ε"				0.887**
Corn	Mass	-0.886**	-0.065	-0.334	-0.428
	Phase shift		-0.395	-0.087	0.144
	ε'			0.866**	0.531
	ε"				0.864**

** Correlation is significant at the 0.01 level.
* Correlation is significant at the 0.05 level.
ε' Dielectric constant.
ε'' Dielectric loss factor.
MC Moisture content.

The significance analysis result was shown in Table 5. P-values greater than 0.05 means no effect was observed in the linear regression model. Therefore, dielectric loss factor and moisture content were removed from the linear regression model for grain mass estimation. Domination of moisture content was imported into the linear model by introducing dielectric constants.

Table 5. Significance analysis of parameters for grain mass model (soybean, canola and corn)

Independence	Soybean	Canola	Corn
Phase shift	0.000	0.000	0.000
Dielectric constants	0.000	0.000	0.021
Dielectric loss factor	0.193	0.409	0.516
Moisture content	0.139	0.343	0.472

2.3.2. Grain Mass Estimation Model

Following the observations of nearly linear relationship between (1) phase shift and grain mass, and (2) dielectric constant and moisture content, by taking into account phase shift and dielectric constant as per model outlined in equation (5), a multiple linear regression model was developed to estimate the grain mass of soybean, canola and corn, respectively. The result of the model in Table 6. showed the linear relationship of grain mass, phase shift and dielectric constant, with the coefficients of determination for soybean, canola, and corn. The result for the soybean sample illustrated that an increase of phase shift by one unit increases the estimation for soybean clean grain mass by 0.04 units when the dielectric constant was remained fixed. When phase shift was held constant, one unit increase of dielectric constant increases the estimation for soybean clean grain mass by 5.249 units. The coefficient of determination (R^2) of the model is 0.976, which indicated that 97.6% of the data fit the model. The result for the canola sample showed that an increase of phase shift by one unit increases the estimation for canola clean grain mass by 0.035 units when the dielectric constant was held constant. When phase shift remained fixed, an increase of dielectric constant by one unit increased the estimation for canola clean grain mass by 4.037 units. The coefficient of determination (R^2) of the model is 0.977, indicating that 97.7% of the data fit the model. For the corn sample, the regression model demonstrated that one unit's increase of phase shift increases the estimation for corn clean grain mass 0.033 units

when the dielectric constant remained fixed. When phase shift was kept constant, an increase of dielectric constant by one unit increased the estimation for corn clean grain mass by 2.704 units. The coefficient of determination (R^2) of the model is 0.989, and this indicates that 98.9% of the data fitted the model. From the regression results, dielectric constant (ε') contributed a large weight to grain mass estimation regression model, which means moisture content interfered with grain mass estimation. By introducing dielectric constant, the interference of moisture content is reasonably included in the regression model of grain mass estimation using phase shift.

Table 6. Regression constants and statistics for grain mass estimation (soybean, canola and corn)

Grain	A_0	a	b	R^2
Soybean	12.391	-0.040	-5.249	0.976
Canola	10.823	-0.035	-4.037	0.977
Corn	7.612	-0.033	-2.704	0.989

0shows the observed grain mass and the estimated grain mass relationship in the sampled grains (soybean, canola and corn). For soybean, the highest average accuracy showed at 12% moisture content with 98.5% accuracy. The lowest average accuracy occurs at 8% moisture content with 85.2% average accuracy. For canola, the average accuracy was largely stable at 92.9%, 93.8%, 97.8%, and94.2% at 8%, 11%, 14% and 17% moisture contents, respectively. For corn, the average accuracy was 93.2%, 94.9%, 97.1% and 93.5% at 12%, 17%, 22% and 27% moisture contents, respectively. At each moisture content, the lowest estimation accuracy happened at 3.5lb of grain mass.

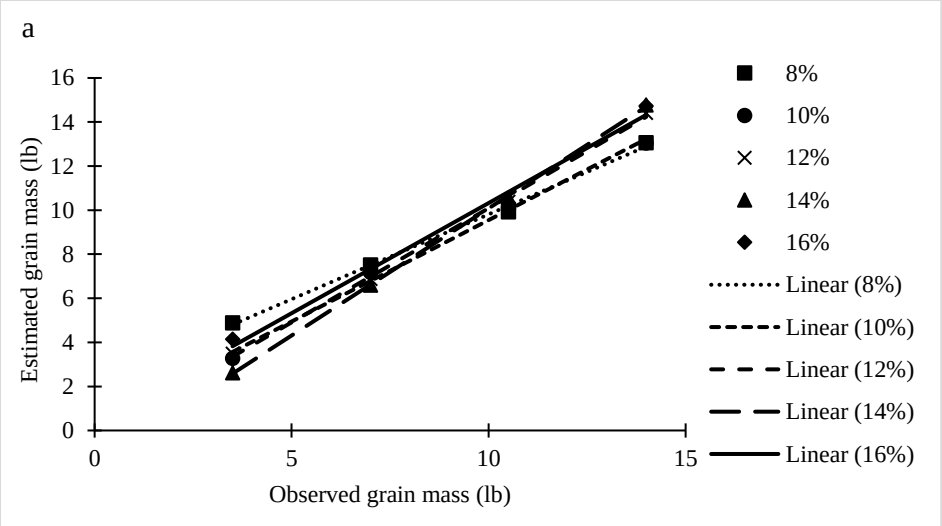

Soybean

Figure 26. Phase shift and dielectric constant dependence of grain mass estimation at indicated moisture contents for (a) soybean (b) canola and (c) corn.

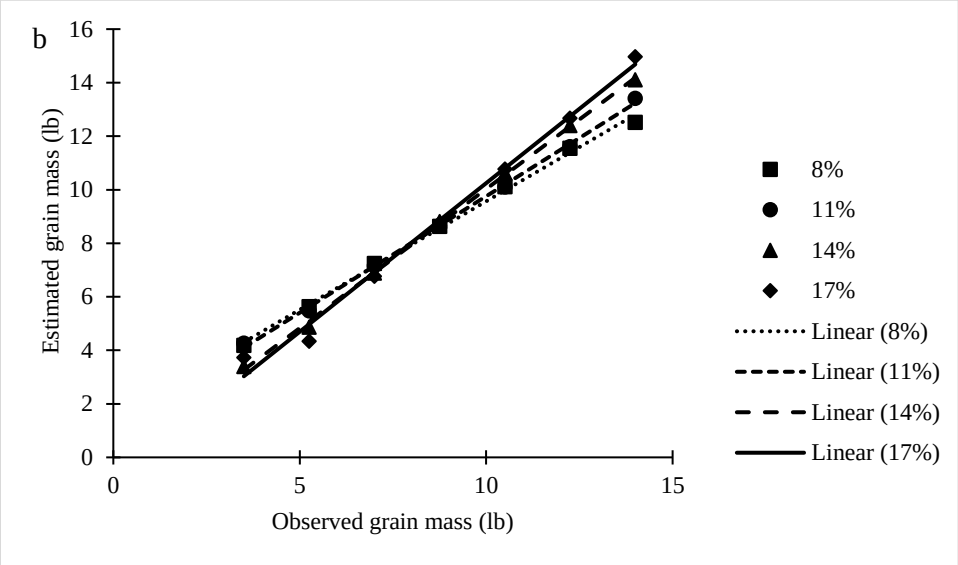

Canola

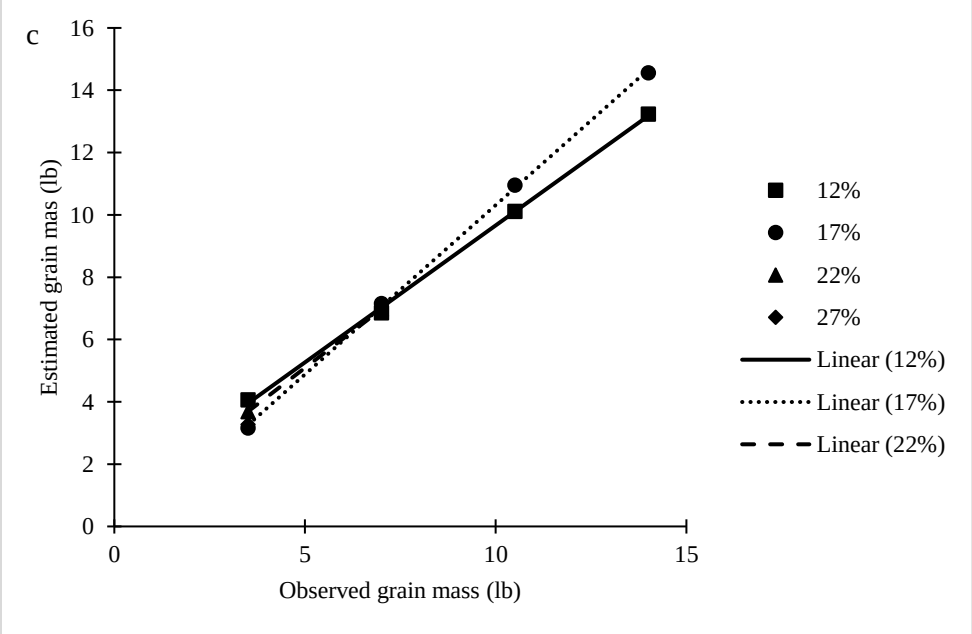

Corn

Figure 26. Phase shift and dielectric constant dependence of grain mass estimation at indicated moisture contents for (a) soybean (b) canola and (c) corn (continued).

2.3.3. Relationship Between Phase Shift Response and Moisture Content

The RF sensing technology has been used in several studies to evaluate grain moisture content. In 2001, Nelson et al. reviewed the techniques and models of sensing moisture using RF dielectric properties (Nelson, Trabelsi et al. 2001). In this study, we took a step further to analyze the relationship between phase shift signal trend with grain mass and the moisture content increments. 0demonstrated the relationship of phase shift with grain mass. Phase shift exhibited a smooth and monotonic trend with the increase of grain mass at different moisture contents. Meanwhile, when the grain mass was kept the same, the phase shifts increased with the moisture content increasing. To some extent, moisture content interfered with phase shifts in grain mass sensing using RF sensing technology. It is difficult to simultaneously solve a sample's unknown mass and moisture content. But, if one of these values is known, then RF sensing can predict the other. Therefore, a reasonable indicator of moisture content in the estimation model should be considered in this study.

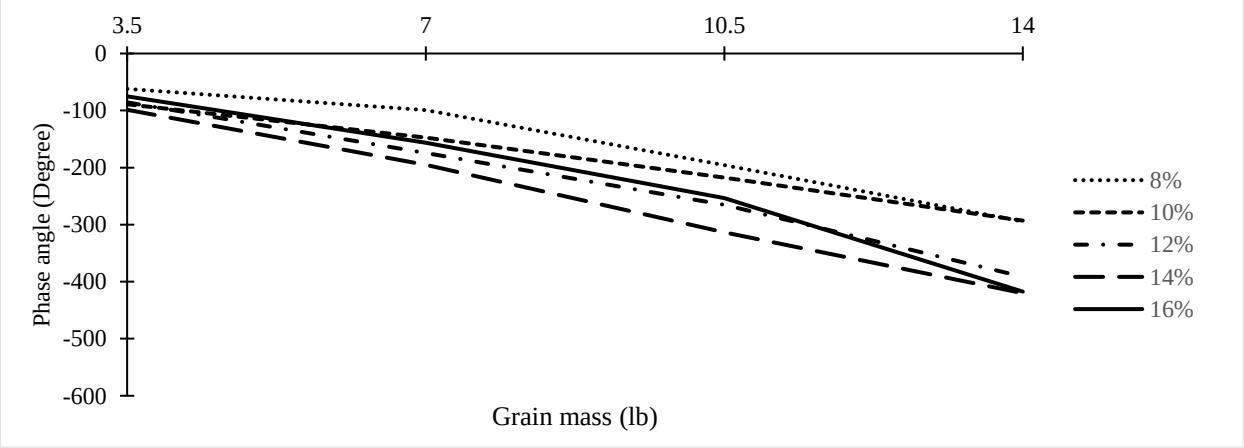

(a) Soybean

Figure 27. Phase shift with grain mass change at different moisture contents
(a) Soybean (b) Canola (c) Corn

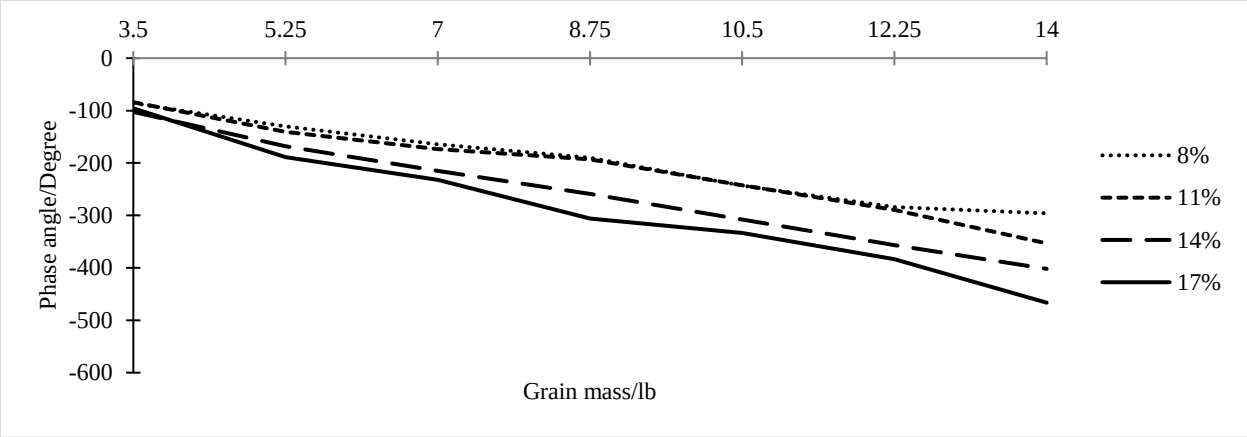

(b) Canola

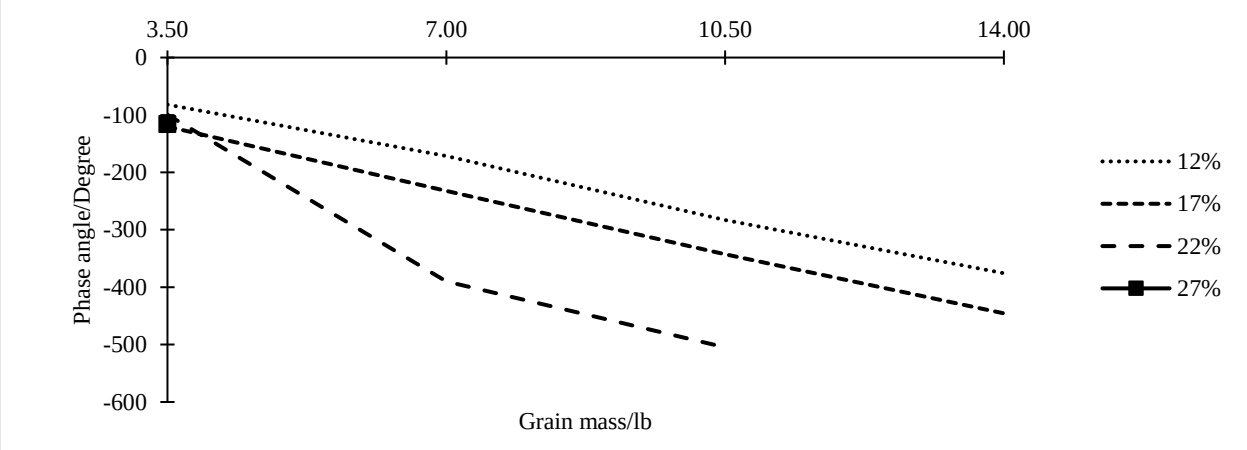

(c) Corn

Figure 27. Phase shift with grain mass change at different moisture contents (a) Soybean (b) Canola (c) Corn (continued).

2.3.4. Relationship Between Dielectric Properties and Moisture Content

Dielectric constant was a key factor for grain moisture content measurement using RF sensing technology (Nelson and Trabelsi 2011). Early measurements of the dielectric properties of many kinds of grains and seeds in the radio frequency or microwave range has revealed high correlations between the grain moisture content and their dielectric properties (Trabelsi and Nelson 2012). According to the statistical analysis above, loss factor (ε'') didn't show high significance in the linear regression model. Therefore, dielectric loss factor wasn't imported in

the regression model. Dielectric constants (ε') were introduced to the grain mass estimation model as a valid indicator of moisture content. To illustrate the relationship between dielectric constant and moisture content, the variance of dielectric constant across the frequency range of 3 to 16 GHz and an average value at different moisture contents were calculated and shown in 0All samples were measured at the same room temperature. Soybean and canola samples were measured at 14lb at different moisture contents and corn samples measured at 3.5lb. The average value of dielectric constant showed an increasing trend with the moisture content increased. When moisture was kept constant, the variance of dielectric constants of soybean and canola didn't demonstrate large changes over the whole testing microwave frequency range, from 3 - 16 GHz. In 0(c), the variance of dielectric constant at 12% and 17% presented a normal value, but at 22% and 27% moisture content, it presented an extremely high value of variance, which is an illustration that attenuation dominant at significant moisture contents. A tentative reason for the phase shift measurements at the higher moisture contents was unknown in the scenarios of this study; the equipment was unable to correctly measure the phase shift due to complete signal loss (high sample attenuation). Therefore, a nonlinear contribution from the loss factor (ε'') will be a tentative objective in the future research. Based on the correlation analysis and significance analysis above, dielectric constant was a valid indicator of moisture content in the grain mass estimation regression model.

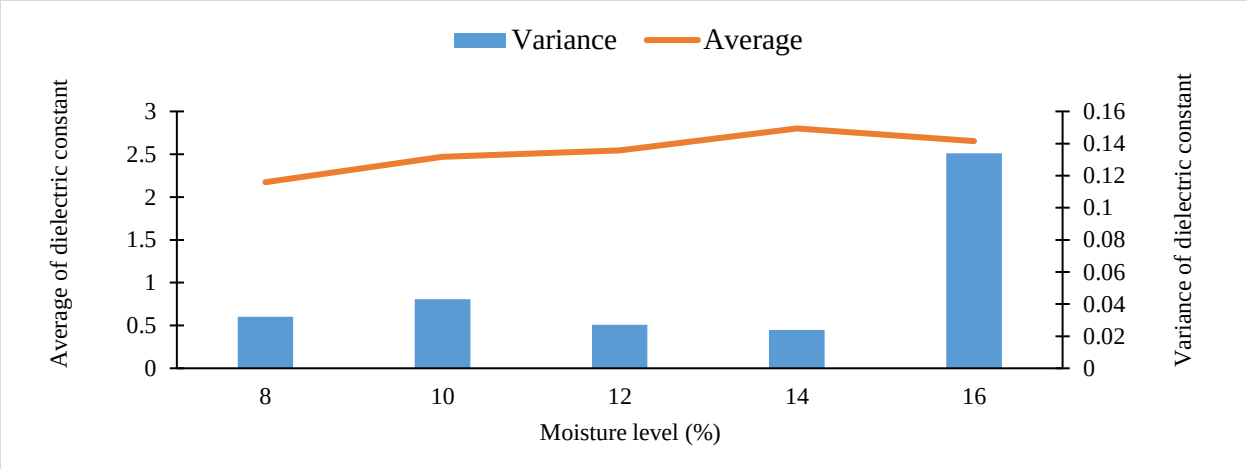

(a) Soybean

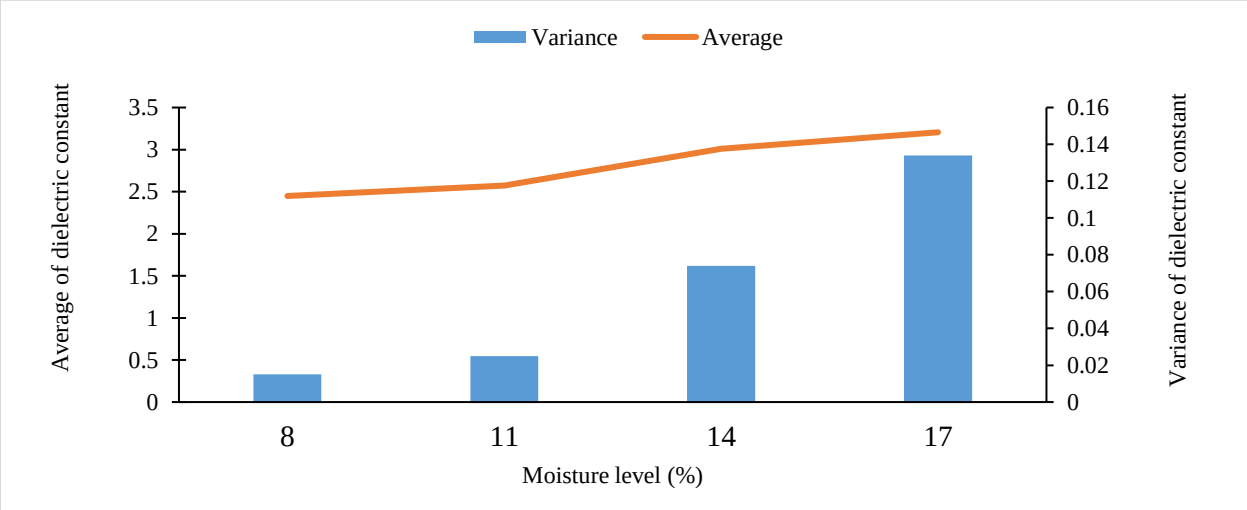

(b) Canola

Figure 28. Variance and average values of dielectric constant at different moisture contents (3 to 16 GHz) (a) Soybean (b) Canola (c) Canola

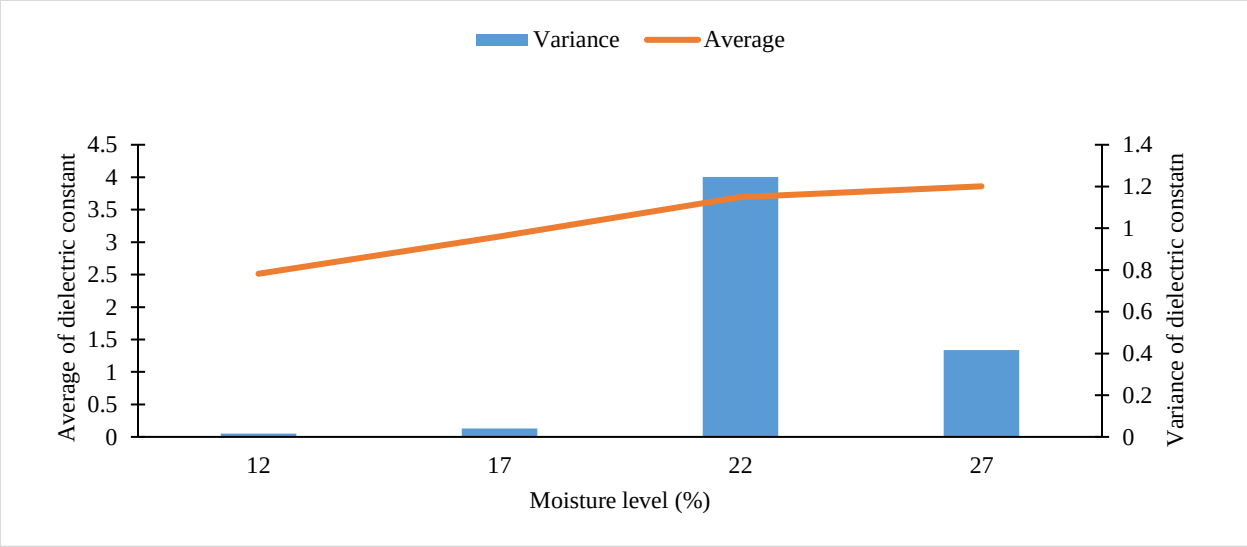

(c) Corn

Figure 28. Variance and average values of dielectric constant at different moisture contents (3 to 16 GHz) (a) Soybean (b) Canola (c) Canola

2.4. Conclusion

In this research, a comprehensive clean grain mass estimation model was established based on the dielectric properties of the grain samples that were extracted by radiofrequency technology. Dielectric constants (ε') and phase shift were inputted as regression model predictors and the mass estimation result with R^2 0.976, 0.977 and 0.989 for soybean, canola and corn samples, respectively. The model result showed promising accuracy for soybean, canola and corn clean grain mass estimation. The results indicated that RF sensing technology has significant potentials to estimate grain mass in precision agricultural yield prediction area. Future research would focus on improving the model using more data and validating the model on dynamic field machinery harvest situation in the field.

REFERENCES

Agilent (2006). Advanced Calibration Techniques for Vector Network Analyzers. Agilent, Agilent.

Andreotti, B., et al. (2013). Granular media: between fluid and solid, Cambridge University Press.

Arslan, S., et al. (2000). "Grain flow measurements with X-ray techniques." Computers and electronics in agriculture **26**(1): 65-80.

Awuah, G. B., et al. (2005). "Inactivation of Escherichia coli K-12 and Listeria innocua in milk using radio frequency (RF) heating." Innovative Food Science & Emerging Technologies **6**(4): 396-402.

Balanis, C. A. (2015). Antenna theory: analysis and design, John wiley & sons.

Chen, W., et al. (2015). "Novel undercoupled radio-frequency (RF) resonant sensor for gaseous ethanol and interferents detection." Sensors and Actuators A: Physical **230**: 63-73.

Chung, S.-O., et al. (2016). "Sensing technologies for grain crop yield monitoring systems: A review." Journal of Biosystems Engineering **41**(4): 408-417.

Clerjon, S. and J.-L. Damez (2009). "Microwave sensing for an objective evaluation of meat ageing." Journal of Food Engineering **94**(3-4): 379-389.

Cohn, H. (2009). "A tight squeeze." Nature **460**(7257): 801-802.

Crawford, E. M. D. G. C., et al. (2020). "American sign language recognition using rf sensing." IEEE Transactions on Human Machine Systems.

Erickson, B. and J. Lowenberg-DeBoer (2019). "2019 Precision agriculture dealership survey." Purdue University.

Fulton, J. P., et al. (2008). "Grain Yield Monitor Flow Sensor Accuracy For Simulated Varying Field Slopes." Applied Engineering in Agriculture **25**(1): 7.

Josephson, C., et al. (2019). "RF soil moisture sensing via radar backscatter tags." arXiv preprint arXiv:1912.12382.

Kadwane, R. (2021). "A Study: Overview to RADAR Systems." Journal of Advanced Research in Wireless, Mobile and Telecommunication **3**(1): 5.

Keysight. "Unknown Thru Calibration." 2020, from http://ena.support.keysight.com/e5071c/manuals/webhelp/eng/measurement/calibration/advanced_calibrations/unknow_thru_calibiration.htm.

Kim, G. and S. Kim (2021). "Design and Analysis of Dual Polarized Broadband Microstrip Patch Antenna for 5G mmWave Antenna Module on FR4 Substrate." IEEE Access **9**: 11.

Knott, E. F. (1993). "Dielectric constant of plastic foams." IEEE transactions on antennas and propagation **41**(8): 1167-1171.

Kong, S. S., et al. (2003). Effects of test table materials for EMC measurement above 1 GHz, IEEE.

Kraszewski, A. W. and S. O. Nelson (2004). "Microwave Permittivity Determination in Agricultural Products." Journal of Microwave Power and Electromagnetic Energy **39**(1): 41-52.

Mario A. de Oliveira, N. V. S. A., Rodolfo N. da Silva,Tony I. da Silva, Jayantha Epaarachchi (2018). "Use of Savitzky-Golay Filter for Performances Improvement of SHM Systems Based on Neural Networks and Distributed PZT Sensors." Sensors **19**(152): 18.

Muqaibel, A., et al. (2003). Ultra wideband material characterization for indoor propagation, IEEE.

Nelson, S. O. (1973). "Electrical properties of agricultural products-A critical review." Transactions of the ASAE **16**(2): 384-0400.

Nelson, S. O. (1987). "Potential agricultural applications for RF and microwave energy." Transactions of the ASAE **30**(3): 818-0831.

Nelson, S. O. (2015). Dielectric Properties of Agricultural Materials and Their Applications. Netherlands, Elsevier Science.

Nelson, S. O. and S. Trabelsi (2011). "Models for the Microwave Dielectric Properties of Grain and Seed." Transactions of the ASABE **54**(2): 5.

Nelson, S. O., et al. (2001). "RF sensing of grain and seed moisture content." IEEE SENSORS **1**(2): 8.

Ng, S. K., et al. (2008). "Determination of added fat in meat paste using microwave and millimetre wave techniques." Meat science **79**(4): 748-756.

Pusch, T., et al. (2019). A reference test setup to support research and development of HPEM testing schemes, IEEE.

Schrock, M. D., et al. (1995). Sensing Grain Yield With a Triangular Elevator. Site-Specific Management for Agricultural Systems. Madison, WI, ASA**:** 14.

Shah, S. A., et al. (2021). "RF Sensing for Healthcare Applications." Backscattering and RF Sensing for Future WirelessCommunication.

Shah, S. A. and F. Fioranelli (2019). "RF sensing technologies for assisted daily living in healthcare: A comprehensive review." IEEE Aerospace and Electronic Systems Magazine **34**(11): 26-44.

Soltani, M. and F. Alimardani (2014). "Moisture content prediction of Iranian wheat using dielectric technique." Journal of Food Science Technology **51**(11): 5.

Tas, E. and F. Pythoud (2017). "Design, implementation, and evaluation of proficiency testing in EMC conducted immunity." IEEE Transactions on Electromagnetic Compatibility **59**(5): 1433-1440.

Thomasson, J. A., et al. (2006). "Optical peanut yield monitor: development and testing." Applied Engineering in Agriculture **22**(6): 809-818.

Trabelsi S, K. A., Nelson, Stuart O. (1998). "A microwave method for on-line determination of bulk density and moisture content of particulate materials." IEEE Transactions of Instrumentation and Measurement **47**(1): 6.

Trabelsi S, K. A., Nelson, Stuart O. (1998). "A mocrowave method for on-line determination of bulk density and moisture content of particulate materials." IEEE Transactions of Instrumentation and Measurement **47**(1): 6.

Trabelsi, S., et al. (2016). "Dielectric properties-based method for rapid and nondestructive moisture sensing in almonds." Journal of Microwave Power and Electromagnetic Energy **50**(2): 11.

Trabelsi, S. and S. O. Nelson (2005). Microwave Dielectric Methods for Rapid, Nondestructive Moisture Sensing in Unshelled and Shelled Peanuts 2005 ASAE Annual International Meeting. Tampa, Florida, US.

Trabelsi, S. and S. O. Nelson (2012). "Microwave Dielectric Properties of Cereal Grains." Transactions of the ASABE **55**(5): 8.

Trabelsi, S., Nelson, Stuart O. (2003). "Free-Space Measurement Of Dielectric Properties Of Cereal Grain And Oilseed At Microwave Frequencies." Measurement Science and Technology **14**(5): 12.

Tucker, C. J., et al. (1979). "Monitoring corn and soybean crop development with hand-held radiometer spectral data." Remote Sensing of Environment **8**(3): 237-248.

Waldron, I. and S. N. Makarov (2006). Measurement of dielectric permittivity and loss tangent for bulk foam samples with suspended ring resonator method, IEEE.

Weberg, C. and R. Striker (2020). "Antenna Bracket." from https://drive.google.com/file/d/1kValCjHffcECElFlCqK5hszK2oDxT9ru/view.